Soft Matter

RAFT-Synthesis and Self-Assembly-Induced Emission of Pendant Diphenylalanine–Tetraphenylethylene Copolymers

Journal:	*Soft Matter*
Manuscript ID	SM-ART-07-2023-000988.R1
Article Type:	Paper
Date Submitted by the Author:	25-Sep-2023
Complete List of Authors:	Yonenuma, Ryo; Yamagata University, Mori, Hideharu; Yamagata University, Graduate School of Organic Materials Science

ARTICLE

RAFT-Synthesis and Self-Assembly-Induced Emission of Pendant Diphenylalanine–Tetraphenylethylene Copolymers

Received 00th January 20xx,
Accepted 00th January 20xx

DOI: 10.1039/x0xx00000x

Ryo Yonenuma,[a] Hideharu Mori[a]

Manipulation of the properties of aggregation-induced emission luminogens (AIEgens) by combining self-assembling motifs has attracted significant interest as a promising approach to develop various advanced materials. In this study, pendant diphenylalanine–tetraphenylethylene (TPE) copolymers exhibiting self-assembly ability and AIE property were synthesized via reversible addition-fragmentation chain-transfer (RAFT) copolymerization. The resulting anionic and non-ionic amphiphilic copolymers with a carbon–carbon main chain bearing diphenylalanine–TPE through-space interactions self-assembled into nanorods and nanofibers, showing blue emissions originating from the aggregation of TPE side chains in the assembled structures. Suitable tuning of the comonomer composition, monomer structure, and environmental conditions (e.g., solvent polarity) enables manipulation of the self-assembled structures, AIE properties, and aggregation-induced circular dichroism by achiral TPE units via through-space interactions with diphenylalanine moieties.

Introduction

Manipulation of the properties of aggregation-induced emission luminogens (AIEgens), which exhibit no emission in solutions but strong emission in the aggregated state,[1-5] by combining self-assembling motifs is attracting increasing interest because such manipulation can be used to develop various advanced materials.[6-21] Recent studies have reported significant progress in the development of AIEgens with a sophisticated design. They also offer a direct link between AIEgens and self-assembling motifs.[6-16] The utilization of noncovalent interactions between AIEgens and self-assembling motifs, such as hydrogen bonding, hydrophobic, and electrostatic interactions, is another promising approach to achieve the desirable self-assembly of AIEgens.[7-12,14-16,18-21] Construction of nano- and microstructures of AIEgens with adjustable fluorescent properties using amino acids or peptides has become one of the most efficient and practical strategies for tuning their fluorescent properties. It can also lead to the development of novel potential applications owing to the merging of the attractive features of AIEgens with amino acid-based properties (e.g., chirality, amphiphilicity, and assembly into hierarchical structures), and the nearly unlimited choice of amino acids (or peptides) and AIE molecules.

Tetraphenylethylene (TPE) exhibits unique structure-driven AIE properties. Therefore, it is used as a representative AIE unit that can be applied to large-area applications such as bioimaging,[22] sensing,[23] and other theragnostic applications.[3] Significant research efforts have been directed toward fabricating TPE–amino acid or TPE–peptide hybrids with unique assembled structures such as helical nano- and microfibers, owing to their useful amino acid-based specific interactions.[7,8,10,15,16] Another attractive feature of AIE–amino acid hybrids is unique aggregation-induced circular dichroism (AICD) that can be obtained by controlling the noncovalent interactions between chiral supramolecules and AIE molecules[7,8,10,18-21] AICD is governed by high-ordered nanostructures, such as twisted or helical nanofibers, obtained by adjusting interactions between the AIE moiety and chiral molecules.[7-12,14-16,18,19]

Diphenylalanine is a unique platform and a versatile building block that can self-assemble into sophisticated nanostructures via noncovalent interactions. In addition to the feasible formation of nano/microtubes,[24-27] nanofibers,[28] and nanowires,[27, 29] diphenylalanine plays a vital role in the development of Alzheimer's disease as it is a part of the core recognition portion of β-amyloid. Thus, the diphenylalanine motif can be employed in a wide range of potential applications involving bioinspired nanomaterials (e.g., antimicrobial activity[30, 31] and biosensors[32, 33]), devices (e.g., piezoelectrics[34, 35]), and material design (e.g., templates[24] and gels[36, 37]). There are also intriguing examples of the application of the properties of AIE moiety-containing diphenylalanine derivatives,[38, 39] such as the formation of microtubes,[40, 41] gels,[42, 43] peptidyl nanostructures,[44] and nanoparticles.[45] In addition, AIE probes have been used to investigate the mechanistic aspects of anti-amyloid compounds by interaction with diphenylalanine.[46]

In addition to small synthetic AIEgens linked covalently with self-assembling motifs, increasing attention has been devoted to AIE polymers containing amino acid or peptide moieties.[15, 17-

[a] Department of Organic Material Science, Graduate School of Organic Materials Science, Yamagata University, 4-3-16, Jonan, Yonezawa City, Yamagata Prefecture 992-8510, Japan

† Footnotes relating to the title and/or authors should appear here.
Electronic Supplementary Information (ESI) available: [details of any supplementary information available should be included here]. See DOI: 10.1039/x0xx00000x

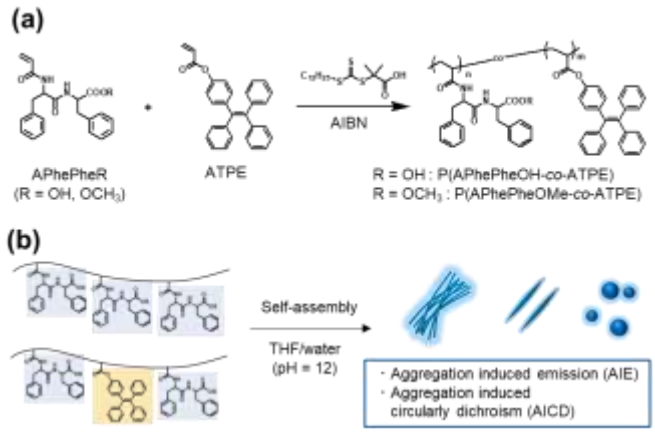

Figure 1. (a) Synthesis of pendant diphenylalanine–TPE copolymers, P(APhePheR-*co*-ATPE) (R = OH, OCH_3). (b) Self-assembly-induced emission and circular dichroism by P(APhePheOH-*co*-ATPE).

[19] Two strategies have been developed for producing TPE–amino acid hybrid polymers: (a) Synthesis of AIE polymers with a TPE unit in the main chain and an amino acid residue (e.g., tyrosine, alanine, and phenylalanine) in the side chain;[18, 19] and (b) synthesis of AIE polymers containing a peptide-based main chain and a TPE side chain.[15] A suitable incorporation of the diphenylalanine motif into a predetermined position in synthetic polymers gives access to a wide range of assembled polymers and bioinspired nanomaterials. A variety of diphenylalanine-containing polymers and nanomaterials have been developed from vinyl monomers, such as *N*-acryloyl-*L*,*L*-diphenylalanine methyl ester (APhePheOMe),[47, 48] a carboxylic acid-containing diphenylalanine acrylamide (*N*-acryloyl-*L*,*L*-diphenylalanine, APhePheOH),[49] and a methacrylate bearing a diphenylalanine-containing tripeptide.[50, 51] Reversible addition-fragmentation chain-transfer (RAFT) polymerization[48, 49] and polymerization-induced self-assembly[50, 51] have been effectively employed for producing well-defined diphenylalanine-containing polymeric materials with sophisticated functions. Other intriguing examples include polymeric gels obtained from diphenylalanine end-modified ethylene glycol-based triblock copolymers,[52] phenylalanine peptide-polyethylene glycol block copolymers,[53] DNA-P(APhePheOMe) hybrid,[54] and diphenylalanine–polymer conjugates consisting of polylactide[55, 56] and polyurethane.[57] Despite their great potential, very few diphenylalanine-containing polymers demonstrating optoelectronic functions, particularly those containing AIEgens, are available. Hence, it is desirable to develop novel dipeptide–AIE hybrid polymers, expand their structural designs, and elucidate the relationship between the assembled structures and AIE properties.

Recently, we developed a diphenylalanine–TPE hybrid monomer with a covalent bond between diphenylalanine (a self-assembling unit) and TPE (AIEgen) and the corresponding homopolymer.[58] The hybrid monomer self-assembled into nanoribbons and fibers with the characteristic AIE and AICD properties. The homopolymer showed molecular-weight-dependent AIE and AICD properties. In this system, an acrylamide is linked covalently with a diphenylalanine–TPE unit. Therefore, the acrylamide/diphenylalanine/TPE ratio was fixed at 1/1/1 in the hybrid monomer unit. However, it is not clear how the diphenylalanine/TPE ratio and through-space interactions affect their self-assembly into a structure that exhibits unique AIE and AICD properties.

Herein, we report the synthesis of pendant-type dipeptide–AIE amphiphilic copolymers bearing diphenylalanine as a self-assembling motif and TPE as an AIEgen with different side chains and tunable compositions (Figure 1). A diphenylalanine-containing acrylamide derivative with a carboxylic acid (APhePheOH) and its methyl ester form (APhePheOMe) are selected, which are then copolymerized with TPE-containing acrylate (ATPE) for the synthesis of anionic and nonionic amphiphilic copolymers by RAFT copolymerization. The first objective of this pendant diphenylalanine–TPE approach is to achieve feasible manipulation of the dipeptide/AIE ratios in the side chains, which can allow the tuning of the through-space interactions between diphenylalanine and TPE and those between diphenylalanine moieties themselves. The second objective is to clarify the effects of monomeric APhePheR structures (R = OH and OCH_3) and environmental conditions (e.g., solvent polarity using THF/water mixtures) on the self-assembled structures, emissions, and AICD behavior.

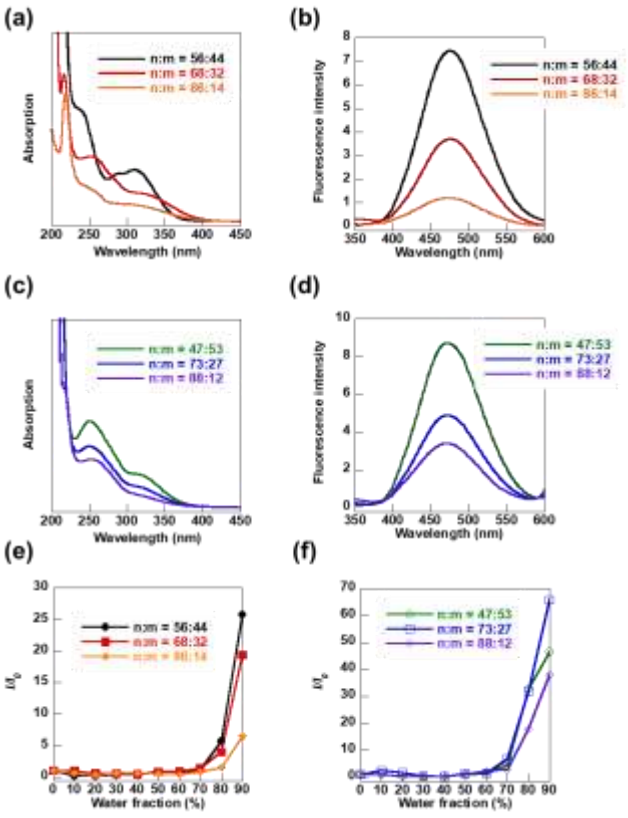

Figure 2. (a, c) UV-vis and (b, d) fluorescence spectra (λ_{ex} = 310 nm) of (a, b) P(APhePheOH-*co*-ATPE)s and (c, d) P(APhePheOMe-*co*-ATPE)s in THF/water (pH = 12) mixture (10/90 vol%). Plots of relative emission peak intensity (I/I_0) of (e) P(APhePheOH-*co*-ATPE)s and (f) P(APhePheOMe-*co*-ATPE)s at 480 nm versus the water fraction of THF/water (pH = 12) mixtures, where I = peak intensity and I_0 = peak intensity in pure THF (final concentration = 0.03 mg/mL).

Table 1. RAFT copolymerization of APhePheOH and ATPE in DMF at 60 °C for 24 h[a)]

Run	[I]/[CTA]/[APhePheOH]/[ATPE]	Conv. (%)[b)] APhePheOH/ATPE	Yield[c)] (%)	M_n[d)] (theory)	M_n[e)] (SEC)	M_w/M_n[e)] (SEC)	APhePheOH:ATPE
1	1/-/50/50	81/<99	72	-	16000	1.82	38:62[b)]
2	1/2/50/50	75/83	74	14500	8300	1.24	40:60[b)]/56:44[f)]
3	1/2/75/25	83/91	70	13400	9000	1.25	63:37[b)]/68:32[f)]
4	1/2/90/10	85/85	72	13600	8500	1.19	86:14[b)]/86:14[f)]

[a)]Monomer concentration = 0.25 g/mL, [M] = [APhePheOH]+[ATPE]; AIBN = 2,2′-azo(isobutyronitrile). [b)]Calculated using ^{1}H NMR spectroscopy in DMSO-d_6. [c)]Diethyl ether/hexane (2:1 v/v)-insoluble fraction. [d)] Theoretical molecular weight (M_n, theory) = ($M_{monomer}$) × [M]/[CTA]$_0$ × yield + (MW of CTA), $M_{monomer}$ = A_1F_1 + A_2F_2 (A = molecular weight, F = molar fraction). [e)]Methylated samples were measured by SEC using PSt standards in DMF (0.01 M of LiBr). [f)]Calculated using elemental analysis.

This study also evaluates the formation of highly ordered structures of these pendant-type copolymers by self-assembly in selective solvents and their assembly-induced emission behaviors using scanning electron microscopy (SEM), transmission electron microscopy (TEM), circular dichroism (CD), and fluorescence measurements. Anionic APhePheOH has two amide groups and one carboxylic acid group, which can contribute to intra- and intermolecular hydrogen bonding and electrostatic interaction in water, whereas the ester linkage in ATPE and APhePheOMe can contribute to hydrogen bonding with the NH unit in the amide units. The hydrophobic interactions between the diphenylalanine–diphenylalanine and diphenylalanine–TPE moieties in the side chains result in a unique self-assembled structure.

Results and discussion

Synthesis of pendant diphenylalanine–TPE copolymers

Two series of pendant copolymers bearing diphenylalanine and TPE units in their side chains, P(APhePheOH-*co*-ATPE)s and P(APhePheOMe-*co*-ATPE)s, respectively, were synthesized by RAFT copolymerization (Figure 1a). Diphenylalanine-containing acrylamide (APhePheOH) provided carboxylic acid-containing amphiphilic copolymers. Nonionic APhePheOMe was used for comparison. TPE-containing acrylate (ATPE) acted as the hydrophobic component to afford anionic and nonionic amphiphilic AIE copolymers. The RAFT copolymerization of APhePheOH and ATPE was conducted in DMF at 60 °C using AIBN as an initiator at [CTA]$_0$/[AIBN]$_0$ = 2 with a trithiocarbonate-type RAFT agent (Table 1, and Figures S3-S4). By adjusting the APhePheOH/ATPE feed ratios (50/50, 75/25, 90/10), the targeted copolymers with pre-determined comonomer compositions (APhePheOH:ATPE = 56:44, 68:32, 86:14) and molecular weights ($M_{n,SEC}$ = 8300–9000) were obtained in reasonable yields (70–74%) after 24 h. The SEC traces of P(APhePheOH-*co*-ATPE)s after the methylation were unimodal with low dispersities in the range of 1.19–1.25 (Figure S7). Similarly, RAFT copolymerizations of APhePheOMe and ATPE at varying feed ratios showed that it is feasible to manipulate the comonomer composition in nonionic pendant copolymers with low dispersities (APhePheOMe:ATPE = 47:53–88:12, M_w/M_n = 1.30–1.40), as shown in Table 2 and Figures S5-S7.

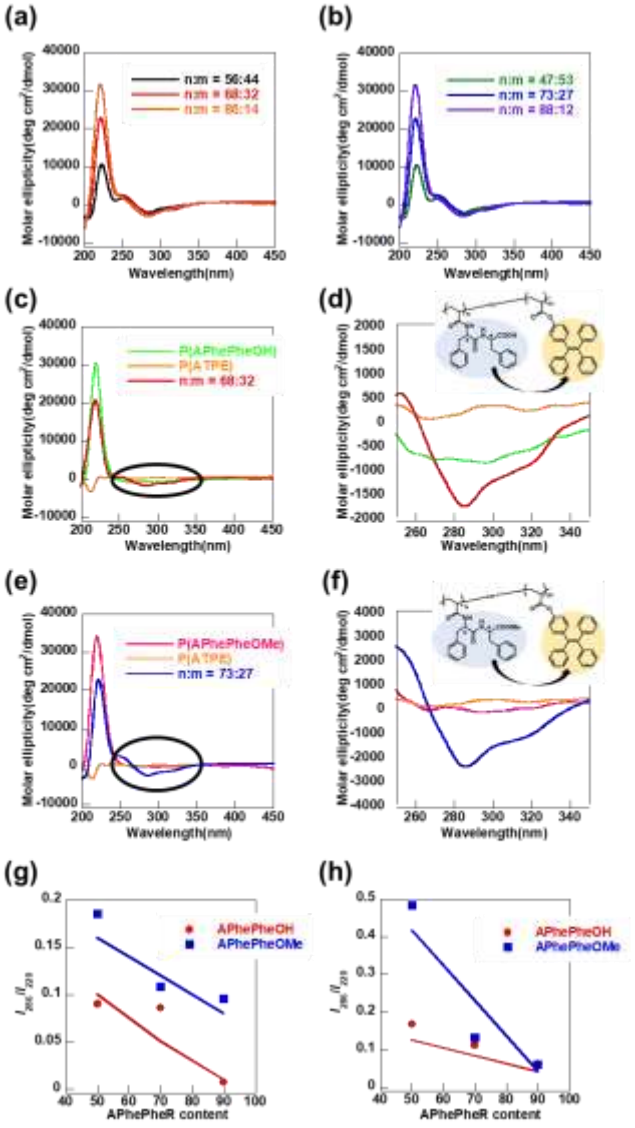

Figure 1. CD spectra of (a) P(APhePheOH-*co*-ATPE)s and (b) P(APhePheOMe-*co*-ATPE)s at different comonomer compositions, and (c, d) comparison of the CD spectra of representative (c, d) P(APhePheOH-*co*-ATPE) and (e, f) P(APhePheOMe-*co*-ATPE) with P(APhePheOH), P(APhePheOMe), and P(ATPE) in THF/water (pH = 12) mixture (10/90 vol%, concentration = 0.03 g/L). Plots of relative CD peak intensity (I_{286}/I_{220}) of P(APhePheOH-*co*-ATPE)s and P(APhePheOMe-*co*-ATPE)s versus APhePheR contents in the THF/water ((g) pH = 12, (h) pH = 7) mixtures (THF/water = 10/90 vol%, concentration = 0.03 mg/mL).

Table 2. RAFT copolymerization of APhePheOMe and ATPE in DMF at 60 °C for 24 h[a)]

Run	[I]/[CTA]/[APhePheOMe]/[ATPE]	Conv. (%)[b)] APhePheOMe/ATPE	Yield[c)] (%)	M_n[d)] (theory)	M_n[e)] (SEC)	M_w/M_n[e)] (SEC)	APhePheOMe:ATPE
1	1/2/50/50	91/97	77	15400	9000	1.39	44:56[b)]/47:53[f)]
2	1/2/75/25	91/95	83	16300	8100	1.40	67:33[b)]/73:27[f)]
3	1/2/90/10	94/88	62	12200	9300	1.30	83:17[b)]/88:12[f)]

[a)]Monomer concentration = 0.25 g/mL, [M] = [APhePheOMe]+[ATPE]; AIBN = 2,2′-azo(isobutyronitrile). [b)]Calculated using ^{1}H NMR spectroscopy in DMSO-d_6. [c)]Diethyl ether/hexane (2:1 v/v)-insoluble fraction. [d)] Theoretical molecular weight (M_n, theory) = ($M_{monomer}$) × [M]/[CTA]$_0$ × yield + (MW of CTA), $M_{monomer} = A_1F_1 + A_2F_2$ (A = molecular weight, F = molar fraction). [e)]Samples were measured by SEC using PSt standards in DMF (0.01 M of LiBr). [f)]Calculated using elemental analysis.

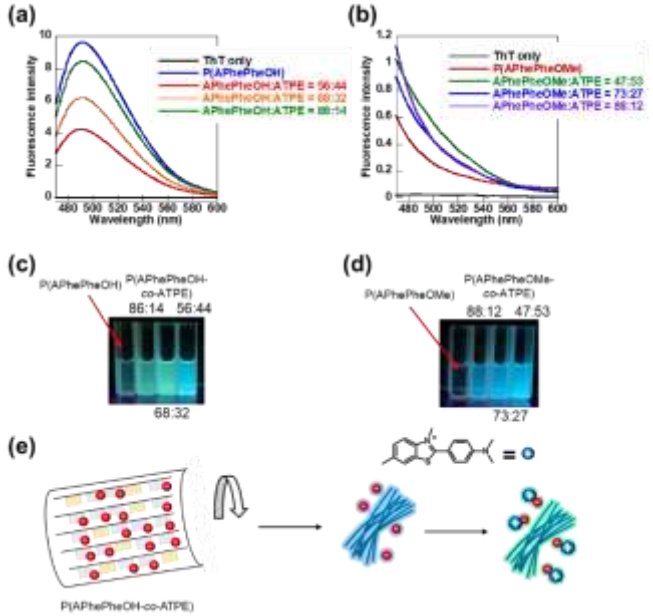

Figure 2. Thioflavin T (ThT) fluorescence of (a) P(APhePheOH-*co*-ATPE)s and (b) P(APhePheOMe-*co*-ATPE)s with different comonomer compositions (λ_{ex} = 450 nm). (c, d) Their photographs in THF/H_2O mixture with ThT (polymer concentration = 0.03 g/L, ThT concentration = 5 μM, λ_{ex} = 365 nm). (c) Postulated binding mechanism of P(APhePheOH-*co*-ATPE) with ThT through electrostatic interactions.

Overall, six pendant copolymers (three anionic and three nonionic) with approximately identical molecular weights ($M_{n,SEC}$ = 8100–9300) and dispersities (M_w/M_n = 1.19–1.40), but with different comonomer compositions, were synthesized and used for further evaluation. In both cases, the polymer yields were slightly lower than those of the monomer conversions (Tables 1 and 2), implying the partial loss of the low molecular weight products during the purification process. To evaluate the comonomer sequence, the monomer reactivity ratios (r_1 and r_2) with APhePheOH and ATPE being designated as M1 and M2 were determined by the copolymerization at different comonomer feeds (Table S1 and Figure S8). Using Fineman–Ross method, r_1 and r_2 values of 0.61 and 4.92 were obtained, suggesting preferable insertion of ATPE at the initial stage of the copolymerizations. The resulting gradient-like copolymers may affect the solution properties and self-assembly behaviour.

P(APhePheOH) exhibits pH-dependent water solubility. It shows good solubility in basic water (pH = 12). However, it is insoluble in acidic and neutral water because of the pH-dependent ionization of a carboxylic acid group in each APhePheOH uni.[49] P(APhePheOH) was also soluble in polar solvents (e.g., DMF, methanol, ethanol, and THF), while P(ATPE) was insoluble in water, methanol, and ethanol (Table S2). Hence, only P(APhePheOH-*co*-ATPE) with a relatively high APhePheOH content (86%) demonstrated reasonable solubility in basic water (pH = 12), methanol, and ethanol. Interestingly, blue luminescence was detected in the basic aqueous solution of P(APhePheOH-*co*-ATPE) (Figure S9). Both anionic P(APhePheOH-*co*-ATPE)s and nonionic P(APhePheOMe-*co*-ATPE)s were soluble in THF, DMF, and acetone, regardless of the comonomer composition (Table S2). Both the pendant copolymers demonstrated good thermal stabilities, exhibiting 5% weight loss above 220 °C, as determined by thermogravimetric analysis (TGA) under nitrogen (Figure S10 and Table S5).

Fluorescent and chiroptical properties of pendant diphenylalanine–TPE copolymers

The fluorescence and chiroptical properties of the pendant diphenylalanine–TPE copolymers were characterized via UV-vis, fluorescence, and CD measurements in THF/water mixtures. An increase in the TPE content of the anionic and nonionic amphiphilic copolymers led to stronger absorbance and fluorescence (Figures 2a-d). It was also demonstrated an increase in the fluorescence intensity with an increase in the ATPE content and water fraction in THF/water (pH = 12) mixtures (Figure 2e-f). The UV-vis spectrum of

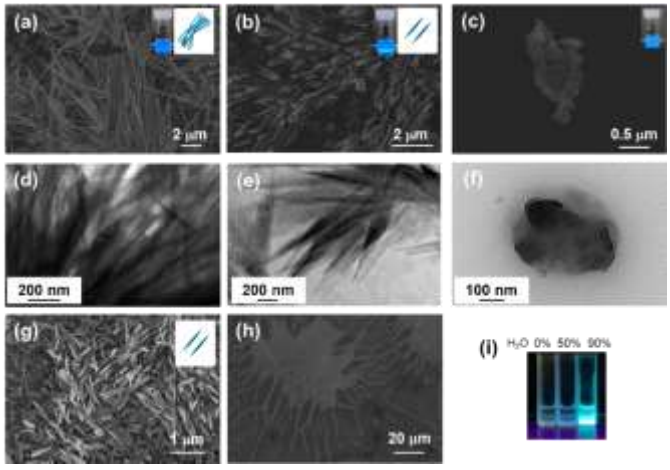

Figure 3. (a-c, g, h) SEM and (d-f) TEM images of P(APhePheOH-*co*-ATPE)s with different comonomer compositions. APhePheOH:ATPE = (a, d) 86:14, (b, e) 68:32, (c, f) 56:44, formed from THF/water (pH = 12) mixture (10/90 vol%). (g, h) SEM images of P(APhePheOH-*co*-ATPE) with high APhePheOH content (86%) formed from different THF/water (pH = 12) mixtures: (g) 50/50 vol%, (h) 100/0 vol% (concentration = 2.0 mg/mL). (i) Photographs of their solutions under UV irradiation (concentration = 2.0 mg/mL, λ_{ex} = 365 nm).

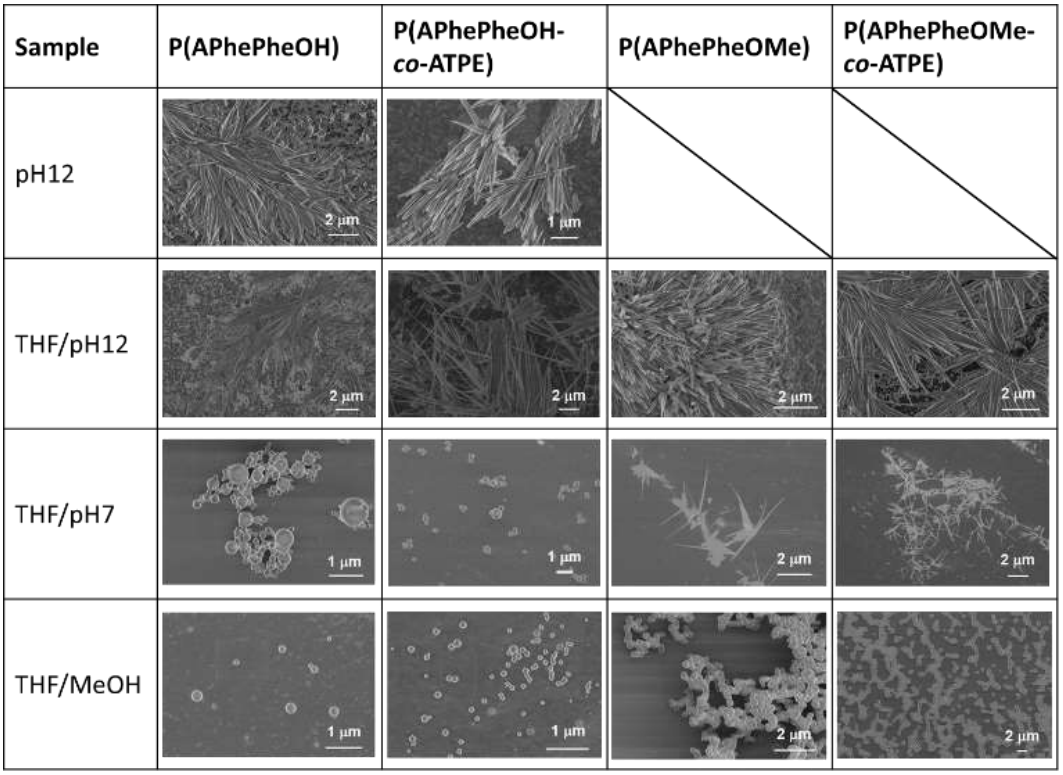

Figure 4. SEM images of P(APhePheOH), P(APhePheOH-*co*-ATPE) with a high APhePheOH content (86%), P(APhePheOMe), and P(APhePheOMe-*co*-ATPE) with a high APhePheOMe content (88%). The samples were prepared from basic water (pH = 12), THF/water (pH = 12) mixtures (10/90 vol%), THF/water (pH = 7) mixture (10/90 vol%), and THF/methanol mixture (10/90 vol%) at 2.0 mg/mL.

P(APhePheOH-*co*-ATPE) with a high ATPE content (44%) in a THF/water (pH = 12) mixture (10/90 vol%) showed absorbances at approximately 250 and 310 nm (Figure 2a), which can be assigned to the phenyl groups of the diphenylalanine unit and the TPE unit, respectively. Peak intensities of these peaks decrease with decreasing ATPE content in the anionic amphiphilic copolymers. When the copolymer was excited at 310 nm, it exhibited blue fluorescence with the maximum emission at approximately 480 nm, which can be attributed to the AIE derived from the aggregated TPE units (Figure 2b).

The fluorescence spectra of the anionic and nonionic amphiphilic copolymers were recorded in THF/water (pH 12) mixtures with different water fractions (Figures S11 and S12). The anionic P(APhePheOH-co-ATPE)s showed negligible emission in THF/water mixtures at water fractions of <70 vol%. In contrast, an increased emission was detected with increased water fractions (80% and 90%), as shown in Figure 2e. A similar tendency was observed for the nonionic P(APhePheOMe-co-ATPE)s (Figure 2f). Both P(APhePheOH-*co*-ATPE) and P(APhePheOMe-*co*-ATPE) showed stronger emissions in THF/neutral water (pH = 7) mixtures than that in THF/basic water (pH = 12) (Figure S13-S14). The fluorescence quantum yields of the anionic and nonionic amphiphilic copolymers were 0.5–1.5 % in THF/water (pH = 12) and 3.0–4.5 % in THF/water (pH = 7) (Table S6). These results suggest that the aggregated states of the TPE unit in the fiber-like structures of both the copolymers formed in THF/water (pH = 12) were less condensed than those in the spherical and acicular structures formed in THF/neutral water (pH = 7).

CD measurements were employed to evaluate the chiroptical and AICD properties of the pendant diphenylalanine–TPE copolymers. In this system, through-space transfer of the chirality of the diphenylalanine motifs into the TPE units located in the side chains was observed. Interestingly, nonionic P(APhePheOMe-*co*-ATPE)s exhibited intensive AICD behavior in contrast to that shown by P(APhePheOH-*co*-ATPE)s in THF/water mixtures. These results are consistent with the AIEgen behavior, suggesting that more condensed states formed from nonionic P(APhePheOMe-*co*-ATPE) compared to those from anionic P(APhePheOH-*co*-ATPE), leading to higher chiral transfer and quantum yields. As shown in Figures 3a and 3b, the CD spectra of the P(APhePheOH-*co*-ATPE)s and P(APhePheOMe-*co*-ATPE)s in the THF/water (pH = 12) mixture (10/90 vol%) exhibit a strong positive peak at 220 nm with an increase in the APhePheR (R = OH and OCH_3) content, suggesting stacking interaction among the aromatic rings of diphenylalanine units.[26, 48, 49] A comparison of the representative CD spectra of the P(APhePheR-*co*-ATPE)s with the corresponding homopolymers, P(APhePheR) and P(ATPE), indicates a strong positive peak at 220 nm in both the copolymers originating from P(APhePheR), regardless of the substitute unit (R = OH or OCH_3, Figures 3c–3f). However, P(ATPE) showed no Cotton effect, as expected, implying an achiral nature. The CD spectrum of P(APhePheR-*co*-ATPE) exhibited a broad negative peak at 280–350 nm, suggesting the through-space transfer of the chirality. Similar chiral transfer and AICD behaviors were observed in amino acid–TPE band small molecules[7, 8] and main-chain type polymers.[18, 19] No significant effect of the water fraction in THF/water mixtures or that of the pH value of water on the chiral

transfer was observed for either copolymer (Figures 3g, 3h, S15, and S16). The relative peak intensities (I_{280}/I_{220}), which correspond to the degree of chiral transfer, were mainly affected by the APhePheR/ATPE composition; a higher ATPE content led to a higher chiral transfer (Figures 3g and 3h). A comparison of the anionic P(APhePheOH-*co*-ATPE)s and the nonionic P(APhePheOMe-*co*-ATPE)s with different comonomer compositions indicated that it is indispensable to have a sufficient amount of diphenylalanine units in order to obtain unique fiber and rod-like assembled structures. Anionic and nonionic APhePheR structures (R = OH or OCH_3) may contribute to the different microscopic locations of TPE and TPE/diphenylalanine units, leading to different assembled structures and emission behaviors.

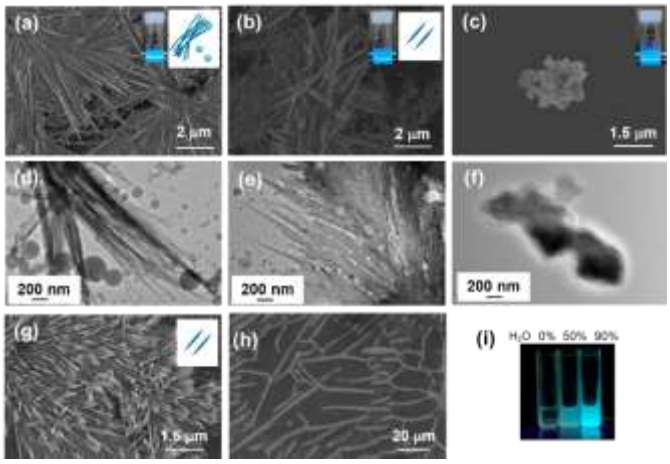

Figure 5. (a-c, g, h) SEM and (d-f) TEM images of P(APhePheOMe-*co*-ATPE)s with different comonomer compositions. APhePheOMe:ATPE = (a, d) 88:12, (b, e) 73:27, (c, f) 47:53, formed from THF/water (pH = 12) mixture (10/90 vol%). (g, h) SEM images of P(APhePheOMe-*co*-ATPE) with a high APhePheOMe content (88%) formed from different THF/water (pH = 12) mixtures: (g) 50/50 vol%, (h) 100/0 vol% (concentration = 2.0 mg/mL). (i) Photographs of their solutions under UV irradiation (concentration = 2.0 mg/mL, λ_{ex} = 365 nm).

Thioflavin T (ThT) fluorescence spectroscopy was used to investigate the secondary structures of the pendant diphenylalanine–TPE copolymers. In the present systems, P(APhePheOH-co-ATPE)s were found to from β-sheet like structure, while different assembled structures were observed in P(APhePheOMe-*co*-ATPE)s. In fibril-containing regions, ThT is frequently used to identify amyloid fibrils, which demonstrate restricted rotation and emission at 490 nm.[53, 59] ThT was added to the THF/water (pH = 7) mixture (10/90 vol%) of both copolymers, followed by absorption and fluorescence measurements (λ_{ex} = 450 nm) (Figures 4 and S17). In the presence of P(APhePheOH-*co*-ATPE)s and P(APhePheOH), ThT exhibited emission at 490 nm. However, ThT itself showed no emission (Figure 4a), suggesting the formation of a β-sheet like structure in the solution. Diphenylalanine-dependent fluorescence was detected, and the intensity decreased with a reduction in the diphenylalanine content of P(APhePheOH-*co*-ATPE)s. Both the nonionic P(APhePheOMe-*co*-ATPE)s and P(APhePheOMe) showed fluorescence peaks at 480 nm (Figures 4b and d), which were apparently distinct from those of the anionic P(APhePheOH-*co*-ATPE)s. P(APhePheOH-*co*-ATPE) has an anionic carboxylic acid in each APhePheOH unit, which can bind to the cationic site of ThT by electronic interaction (Figure 4e).

Assembled structures and AIE properties of P(APhePheOH-*co*-ATPE)

SEM and TEM measurements were conducted to confirm the self-assembled structures of the pendant diphenylalanine–TPE copolymers. Different morphologies (e.g., fibers, nanorods, and spherical particles) were obtained, which were mainly governed by the copolymer composition (APhePheR/ATPE ratio) and environmental conditions (e.g., solvent polarity, including THF/water ratio, water pH value, and solvent concentration). As an efficient strategy to form self-assembled structures from diphenylalanine and its derivatives, the dilution of a stock solution dissolved in a good solvent (e.g., hexafluoroisopropanol) by a poor solvent (e.g., water) was frequently employed.[24] Both P(APhePheOH-*co*-ATPE) and P(APhePheOMe-*co*-ATPE) were insoluble in hexafluoroisopropanol owing to the presence of the TPE moiety. Hence, THF was selected as a good solvent that exhibits universal solubility for both the copolymers, independent of the comonomer composition. The copolymer was initially dissolved in THF at a concentration of 20 mg/mL, followed by the dilution with a basic water (pH 12), affording a mixed solution (2.0 mg/mL), and the resulting mixed solution was used for the sample preparation. Figure 5 shows the representative SEM and TEM images of the assembled structures of P(APhePheOH-*co*-ATPE)s prepared using a THF/water (pH = 12) solution (10/90 vol%, final concentration = 2.0 mg/mL). The photographs of the emission behavior in the mixed solutions are also given. As depicted in the SEM images (Figures 5a and b), the amphiphilic copolymers with relatively higher APhePheOH contents (86–68%) had nanofiber-like assembled structures with blue emission that is a few micrometers long and <500 nm wide. Similar nanofiber-like crystals were observed in the TEM images (Figures 5d and e). The higher APhePheOH content of the copolymers increases their length to 10 μm (Figure 5a), which suggests that the nanorods change to nanofibers on increasing the number of APhePheOH moieties in the copolymers. Similarly, fiber-like structures were observed in the SEM images of the P(APhePheOH) samples prepared using a THF/water (pH = 12) solution (10/90 vol%) and basic water, as illustrated in Figure 6. These structures are comparable to the morphologies of P(APhePheOH) sample prepared using a hexafluoroisopropanol/basic water reported in our previous study.[49] These results imply that the ordered structures of P(APhePheOH-*co*-ATPE)s originate from the specific interactions of APhePheOH moieties. Occasionally, fractal structures can be seen in the SEM images (Figure S18). P(APhePheOH-*co*-ATPE), with a low APhePheOH content (56%), shows agglomerated structures without any assembled features (Figures 5c and f).

Next, we evaluate the effects of the water fraction in THF/water mixtures, their concentrations, and water pH values on the assembled structures and AIE behavior of P(APhePheOH-*co*-ATPE) with a high APhePheOH content (86%). As shown in Figure 5g, short nanofiber-like structures can be seen when the amphiphilic copolymer sample is prepared from a THF/water (pH 12) mixture (50/50 vol%). In the sample prepared from THF, no assembled structures with negligible emissions were

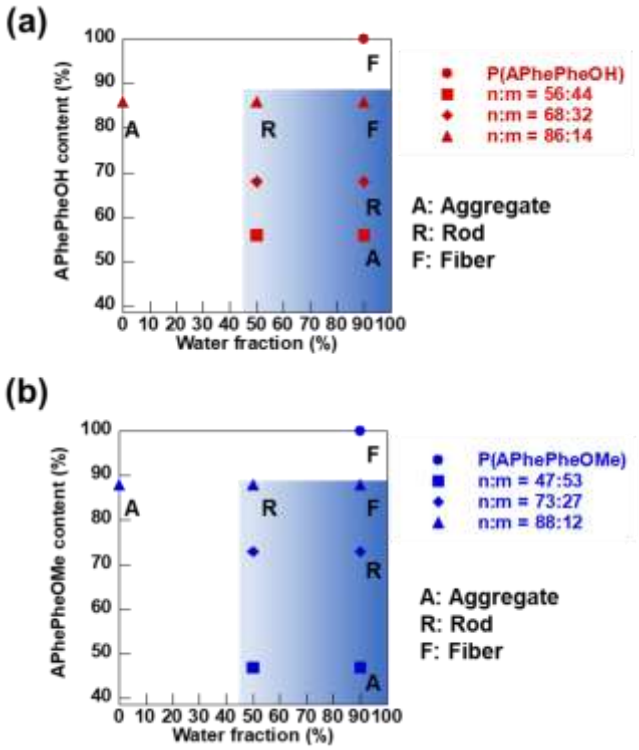

Figure 8. Self-assembly and AIE relationship between APhePheR content and the water fraction of THF/water (pH = 12) mixtures of (a) P(APhePheOH-*co*-ATPE)s and (b) P(AhePheOMe-*co*-ATPE)s (conc. = 2.0 mg/mL). Morphologies were confirmed by SEM, where A, R, and F denote aggregate, rod, and fiber, respectively. AIE behavior was observed in the blue color area shown in (a) and (b).

detected (Figures 5h and i), whereas longer and wider fibers tightly bound together were obtained when basic water (pH = 12, Figure 5) was used. This implies that a poor solvent (basic water in this system) can be acted as a selective solvent, showing a reasonable solubility only for APhePheOH unit, leading to the formation of fiber-like assembled structures. The solution was further diluted with a THF/water (pH = 12) mixture (10/90 vol%, concentration = 1.0 mg/mL). A broom-like structure was obtained from P(APhePheOH-*co*-ATPE) (Figure S19). Spherical structures were obtained when THF/water (pH = 7 and 5) and THF/methanol mixtures (10/90 vol%) were used (Figures 6 and S20). Spherical structures with flexible fiber-like structures were obtained from THF/water (pH 10) and THF/buffer (pH 7.4) mixtures, whereas agglomerated structures were obtained from the THF/water (pH 3) mixture (10/90 vol%, Figure S20). The self-assembled structures of the diphenylalanine derivatives were reported to be greatly affected by pH values.[60-63] Therefore, diphenylalanine derivatives were employed for obtaining pH-sensitive hydrogels,[60] fluorescent pH probes,[61] and pH-responsible biomolecular logic systems.[62] Saiami et al. reported that a diphenylalanine-modified dansyl derivative exhibited pH-sensitive emission in aqueous solutions in a wide pH range (1–13).[61] Thordarson et al. also demonstrated the tuning ability of the self-assembly of heterocyclic modified dipeptides at high pH.[64] Gazit et al. reported on the stability of dipeptide-based nanoparticles under acidic (10% trifluoroacetic acid) and basic (1 M NaOH) aqueous conditions and the importance of structural stability for the nanofabrication and industrial applications.[25] In our system, the carboxylic acid in the APhePheOH unit of the pendant copolymers is fully ionized and present as a negatively charged unit in basic water (pH = 12) and THF/water (pH = 12) mixtures with high water fractions. Under these conditions, APhePheOH unit is located at the outermost surface of the ordered structures, and the electrostatic repulsion between the carboxylate anion and/or amide–amide and amide–ester hydrogen bonds may affect the self-assembly of amphiphilic P(APhePheOH-*co*-ATPE)s.

Structural effects and postulated assembly mechanisms

To address the effect of the carboxylic acid present in the APhePheOH unit, the assembled structures of nonionic P(APhePheOMe-*co*-ATPE)s were evaluated. The structural difference in the diphenylalanine monomer unit (APhePheR, R = OH or OCH_3) had only a minor impact on the assembled structures, whereas they had substantial effects on the AIE and AICD owing to the microscopic localization of the TPE itself and that of the TPE/diphenylalanine units in the assembled structures. This may be because the hydrophobic interactions between APhePheR–APhePheR, APhePheR–ATPE, and ATPE–ATPE were predominant compared to those between the hydrogen bonds and electrostatic interactions for the formation of the assembled structures.

Similar to the anionic P(APhePheOH-*co*-ATPE)s, ordered structures were obtained on increasing the number of APhePheOMe moieties in the THF/water (pH = 12) mixture (10/90 vol%) (Figures 7a and b). Spherical structures (diameter = 100–300 nm) were occasionally detected along with nanorods and nanofibers (Figures 7d and e), suggesting that P(APhePheOMe-*co*-ATPE) was more aggregated than

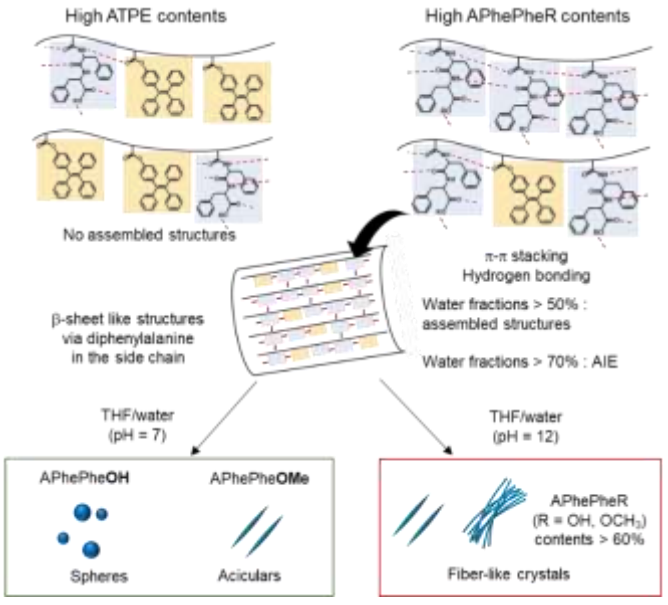

Figure 9. Schematic illustration of the postulated assembled mechanisms of P(APhePheOH-*co*-ATPE) and P(APhePheOMe-*co*-ATPE) in THF/water mixtures at different water pH values.

P(APhePheOH-*co*-ATPE). As shown in Figures 7c and f, P(APhePheOMe-*co*-ATPE) with a low APhePheOMe content (47%) exhibited only agglomeration. When the ratio of the poor solvent (basic water) was increased, the copolymer self-assembled from nanorods into nanofibers (Figures 7a and g); in contrast, no assembled structure was obtained in THF (Figure 7h). As expected, the blue emission of the nonionic copolymers in THF/water (pH = 12) mixtures increased on increasing the water fraction (Figure 7i). Flexible fibers were observed when the P(APhePheOMe-*co*-ATPE) sample was prepared from a dilute solution (concentration = 1.0 mg/mL, THF/water (pH = 12) mixture (10/90 vol%)) (Figure S21). In contrast, no fiber-like structures were detected in the samples prepared from THF/water (pH = 7) and THF/methanol mixtures (10/90 vol%, concentration = 2.0 mg/mL, Figure 6).

Figure 8 summarize the self-assembly and AIE relationship between APhePheR content and the water fraction of THF/water (pH = 12) mixtures of P(APhePheOH-*co*-ATPE)s and P(AhePheOMe-*co*-ATPE)s. Both the anionic and nonionic amphiphilic copolymers with higher diphenylalanine contents (APhePheR >60%) can provide nanofibers that exhibit a strong blue emission owing to the aggregation of TPE moieties in THF/water (pH = 12) mixtures with higher water fractions (≥50%), regardless of the diphenylalanine-based monomer structures (R = OH and OCH_3 in APhePheR). A control experiment using ^1H NMR measurement suggested that the ester group in APhePheOMe unit in the nonionic copolymer was maintained without unfavorable side reactions (e.g., hydrolysis) even under the treatment in THF/water (pH = 12) mixture (Figure S22).

Figure 9 illustrates the postulated assembly mechanisms of both the copolymers. ThT fluorescence showed that the poly(APhePheOH-*co*-ATPE)s form β-sheet structures via intermolecular interaction between the diphenylalanine moieties, depending on the APhePheOH content. The copolymers with high APhePheOH contents (68–86%) self-assemble into β-sheet structures, which can then extend from nanorods to nanofibers owing to an increase in the number of diphenylalanine moieties of the copolymers. In this step, diphenylalanine-based hydrophobic interactions and amide–hydrogen bonds were predominant, leading to the formation of β-sheet structures. In the next step, fiber-like crystals and acicular and spherical structures were formed, depending on the environmental conditions (e.g., THF/water fraction and water pH). In contrast, in P(APhePheOH-*co*-ATPE) with a low APhePheOH content (<56%), the intra- and intermolecular hydrogen bonding between the ester unit in the ATPE unit and the amide groups in APhePheOH are predominant, leading to the suppression of the diphenylalanine-based self-assembly.

Conclusion

Herein we reported the synthesis and self-assembly-induced emission of pendant diphenylalanine–TPE copolymers. P(APhePheOH-*co*-ATPE)s with a high APhePheOH content can self-assemble into nanorods and nanofibers in THF/water (pH = 12) mixtures with an increase in the water fraction (>70%). The tunable emission and AICD properties and assembled structures achieved by precise manipulation of the diphenylalanine–TPE composition stress upon the advantages of the controlled copolymerization strategy used in this study. In addition to the intrinsic hydrophobic interactions between diphenylalanine, diphenylalanine–TPE, hydrogen bondings between the amide and ester linkages and electrostatic interactions also play crucial roles in self-assembly and chiral transfer in the side chains. Both copolymers exhibited AICD properties owing to the TPE units by interacting with the diphenylalanine moieties. They may also exhibit circularly polarized luminescence. This study showed that obtaining self-assembly-induced emissions from novel pendant copolymers bearing phenylalanine and TPE units in the side chains and understanding their structural design and principles are valuable for developing unique dipeptide–AIE hybrid polymers with various potential applications.

Conflicts of interest

There are no conflicts to declare.

Acknowledgements

This work was supported by JST, the establishment of university fellowships towards the creation of science technology innovation, Grant Number JPMJFS2104.

Notes and references

1. Y. Hong, J. W. Y. Lam and B. Z. Tang, *Chem. Soc. Rev.*, 2011, **40**, 5361-5388.
2. J. Luo, Z. Xie, J. W. Y. Lam, L. Cheng, H. Chen, C. Qiu, H. S. Kwok, X. Zhan, Y. Liu, D. Zhu and B. Z. Tang, *Chem. Commun.*, 2001, **18**, 1740-1741.
3. X. Cai and B. Liu, *Angew. Chem. Int. Ed. Engl.*, 2020, **59**, 9868-9886.
4. R. Hu, A. Qin and B. Z. Tang, *Prog. Polym. Sci.*, 2020, **100**, 101176.
5. Q. Wan, Q. Huang, M. Liu, D. Xu, H. Huang, X. Zhang and Y. Wei, *Appl. Mater. Today*, 2017, **9**, 145-160.
6. S. Zhang, J. M. Yan, A. J. Qin, J. Z. Sun and B. Z. Tang, *Chin. Chem. Lett.*, 2013, **24**, 668-672.
7. H. Li, J. Cheng, Y. Zhao, J. W. Y. Lam, K. S. Wong, H. Wu, B. S. Li and B. Z. Tang, *Mater. Horiz.*, 2014, **1**, 518-521.
8. H. Li, X. Zheng, H. Su, J. W. Y. Lam, K. Sing Wong, S. Xue, X. Huang, X. Huang, B. S. Li and B. Z. Tang, *Sci. Rep.*, 2016, **6**, 19277.
9. H. Li, S. Xue, H. Su, B. Shen, Z. Cheng, J. W. Lam, K. S. Wong, H. Wu, B. S. Li and B. Z. Tang, *Small*, 2016, **12**, 6593-6601.
10. B. S. Li, R. Wen, S. Xue, L. Shi, Z. Tang, Z. Wang and B. Z. Tang, *Mater. Chem. Front.*, 2017, **1**, 646-653.
11. G. Huang, R. Wen, Z. Wang, B. S. Li and B. Z. Tang, *Mater. Chem. Front.*, 2018, **2**, 1884-1892.
12. S. P. Goskulwad, M. A. Kobaisi, D. D. La, R. S. Bhosale, M. Ratanlal, S. V. Bhosale and S. V. Bhosale, *Chem. Asian J.*, 2018, **13**, 3947-3953.

13. B. S. Li, X. Huang, H. Li, W. Xia, S. Xue, Q. Xia and B. Z. Tang, *Langmuir*, 2019, **35**, 3805-3813.
14. S. P. Goskulwad, V. G. More, M. A. Kobaisi, R. S. Bhosale, D. D. La, F. Antolasic, S. V. Bhosale and S. V. Bhosale, *ChemistrySelect*, 2019, **4**, 2626-2633.
15. Y. Shi, G. Yin, Z. Yan, P. Sang, M. Wang, R. Brzozowski, P. Eswara, L. Wojtas, Y. Zheng, X. Li and J. Cai, *J. Am. Chem. Soc.*, 2019, **141**, 12697-12706.
16. Y. Wang, D. Niu, G. Ouyang and M. Liu, *Nat. Commun.*, 2022, **13**, 1710.
17. X. Liu, J. Jiao, X. Jiang, J. Li, Y. Cheng and C. Zhu, *J. Mater. Chem. C*, 2013, **1**, 4713-4719.
18. Q. Liu, Q. Xia, S. Wang, B. S. Li and B. Z. Tang, *J. Mater. Chem. C*, 2018, **6**, 4807-4816.
19. Q. Liu, Q. Xia, Y. Xiong, B. S. Li and B. Z. Tang, *Macromolecules*, 2020, **53**, 6288-6298.
20. Q. Li, J. Zhang, Y. Wang, G. Zhang, W. Qi, S. You, R. Su and Z. He, *Nano Lett.*, 2021, **21**, 6406-6415.
21. J. Li, X. Peng, D. Chen, S. Shi, J. Ma and W. Y. Lai, *ACS Macro Lett.*, 2022, **11**, 1174-1182.
22. S. Xie, A. Y. H. Wong, R. T. K. Kwok, Y. Li, H. Su, J. W. Y. Lam, S. Chen and B. Z. Tang, *Angew. Chem. Int. Ed. Engl.*, 2018, **57**, 5750-5753.
23. A. Qin, J. W. Y. Lam, L. Tang, C. K. W. Jim, H. Zhao, J. Sun and B. Z. Tang, *Macromolecules*, 2009, **42**, 1421-1424.
24. M. Reches and E. Gazit, *Science*, 2003, **300**, 625-627.
25. M. Reches and E. Gazit, *Nano Lett.*, 2004, **4**, 581-585.
26. L. Adler-Abramovich, M. Reches, V. L. Sedman, S. Allen, S. J. B. Tendler and E. Gazit, *Langmuir*, 2006, **22**, 1313-1320.
27. J. Kim, T. H. Han, Y. I. Kim, J. S. Park, J. Choi, D. G. Churchill, S. O. Kim and H. Ihee, *Adv. Mater.*, 2010, **22**, 583-587.
28. R. Huang, W. Qi, R. Su, J. Zhao and Z. He, *Soft Matter*, 2011, **7**, 6418-6421.
29. T. H. Han, J. Kim, J. S. Park, C. B. Park, H. Ihee and S. O. Kim, *Adv. Mater.*, 2007, **19**, 3924-3927.
30. S. L. Porter, S. M. Coulter, S. Pentlavalli, T. P. Thompson and G. Laverty, *Acta Biomater.*, 2018, **77**, 96-105.
31. Y. C. Tsai, C. C. Tang, H. H. Wu, Y. S. Wang and Y. F. Chen, *Int. J. Pept. Res. Ther.*, 2020, **26**, 1107-1114.
32. M. Yemini, M. Reches, J. Rishpon and E. Gazit, *Nano Lett.*, 2005, **5**, 183-186.
33. M. Yemini, M. Reches, E. Gazit and J. Rishpon, *Anal. Chem.*, 2005, **77**, 5155-5159.
34. V. Nguyen, R. Zhu, K. Jenkins and R. Yang, *Nat. Commun.*, 2016, **7**, 13566.
35. S. Safaryan, V. Slabov, S. Kopyl, K. Romanyuk, I. Bdikin, S. Vasilev, P. Zelenovskiy, V. Y. Shur, E. A. Uslamin, E. A. Pidko, A. V. Vinogradov and A. L. Kholkin, *ACS Appl. Mater. Interfaces*, 2018, **10**, 10543-10551.
36. P. Zhu, X. Yan, Y. Su, Y. Yang and J. Li, *Chem. Eur. J.*, 2010, **16**, 3176-3183.
37. N. A. Dudukovic and C. F. Zukoski, *Langmuir*, 2014, **30**, 4493-4500.
38. Z. Gan and H. Xu, *Macromol. Rapid Commun.*, 2017, **38**, 1700370.
39. C. Diaferia, E. Rosa, E. Gallo, G. Morelli and A. Accardo, *Chem. Eur. J.*, 2023, **29**, e202300661.
40. N. Na, X. Mu, Q. Liu, J. Wen, F. Wang and J. Ouyang, *Chem. Commun.*, 2013, **49**, 10076-10078.
41. C. Fu, D. Zhang, G. Xu, X. Deng, M. Liu, Y. Deng, W. Lu, C. Chen, Y. Ruan and Y. Yu, *J. Lumin.*, 2021, **238**, 118320.
42. F. Sun, G. Zhang and D. Zhang, *Chin. Sci. Bull.*, 2012, **57**, 4284-4288.
43. A. M. Castilla, B. Dietrich and D. J. Adams, *Gels*, 2018, **4**, 17.
44. Z. Gan, M. Meng, Y. Di and S. Huang, *New J. Chem.*, 2016, **40**, 1970-1973.
45. J. Kong, Y. Wang, W. Qi, R. Su and Z. He, *ACS Appl. Mater. Interfaces*, 2019, **11**, 15401-15410.
46. B. Koshti, V. Kshtriya, C. Nardin and N. Gour, *ACS Chem Neurosci*, 2021, **12**, 2851-2864.
47. H. Skaat, R. Chen, I. Grinberg and S. Margel, *Biomacromolecules*, 2012, **13**, 2662-2670.
48. J. L. Warren, P. A. Dykeman-Bermingham and A. S. Knight, *J. Am. Chem. Soc.*, 2021, **143**, 13228-13234.
49. R. Yonenuma, A. Ishizuki, K. Nakabayashi and H. Mori, *J. Polym. Sci., Part A: Polym. Chem.*, 2019, **57**, 2562-2574.
50. T. P. T. Dao, L. Vezenkov, G. Subra, M. Amblard, M. In, J. F. Le Meins, F. Aubrit, M. A. Moradi, V. Ladmiral and M. Semsarilar, *Macromolecules*, 2020, **53**, 7034-7043.
51. T. P. T. Dao, L. Vezenkov, G. Subra, V. Ladmiral and M. Semsarilar, *Polym. Chem.*, 2021, **12**, 113-121.
52. H. A. Kim, H. J. Lee, J. H. Hong, H. J. Moon, D. Y. Ko and B. Jeong, *Biomacromolecules*, 2017, **18**, 2214-2219.
53. V. Castelletto and I. W. Hamley, *Biophys. Chem.*, 2009, **141**, 169-174.
54. C. J. Kim, J. E. Park, X. Hu, S. K. Albert and S. J. Park, *ACS Nano*, 2020, **14**, 2276-2284.
55. S. K. Murase, N. Haspel, L. J. del Valle, E. A. Perpète, C. Michaux, R. Nussinov, J. Puiggalí and C. Alemán, *RSC Adv.*, 2014, **4**, 23231-23241.
56. E. Mayans, S. K. Murase, M. M. Pérez-Madrigal, C. Cativiela, C. Alemán and J. Puiggalí, *Macromol. Chem. Phys.*, 2018, **219**, 1800168.
57. F. Zhang, R. Wang, Y. He, W. Lin, Y. Li, Y. Shao, J. Li, M. Ding, F. Luo, H. Tan and Q. Fu, *J. Mater. Chem. B*, 2018, **6**, 4326-4337.
58. R. Yonenuma and H. Mori, *Polym. Chem.*, 2023, **14**, 1469-1477.
59. M. Biancalana and S. Koide, *Biochim. Biophys. Acta Proteins Proteom.*, 2010, **1804**, 1405-1412.
60. C. Tang, A. M. Smith, R. F. Collins, R. V. Ulijn and A. Saiani, *Langmuir*, 2009, **25**, 9447-9453.
61. G. Zhang, L. Zhang, H. Rao, Y. Wang, Q. Li, W. Qi, X. Yang, R. Su and Z. He, *J. Colloid Interface Sci.*, 2020, **577**, 388-396.
62. Y. Wang, L. Zeng, J. Zhou, B. Jiang, L. Zhao, C. Wang and B. Xu, *Spectrochim. Acta A Mol. Biomol. Spectrosc.*, 2019, **223**, 117348.
63. J. Li, C. Xiao, W. Wei, R. Xiao, H. Yao and H. Liu, *ACS Appl. Mater. Interfaces*, 2021, **13**, 36632-36643.
64. A. D. Martin, J. P. Wojciechowski, A. B. Robinson, C. Heu, C. J. Garvey, J. Ratcliffe, L. J. Waddington, J. Gardiner and P. Thordarson, *Sci Rep*, 2017, **7**, 43947.